ARCHITECTURAL RESEARCH, Vol. 8, No. 1(June 2006), pp. 47-56

Post-buckling Behavior of Tapered Columns under a Combined Load using Differential Transformation

Yeong Chan Yoo

Department of Architectural Engineering, College of Engineering, Andong National University

Abstract

In this research, the analysis of post-buckling behavior of tapered columns has been performed under a combined load of uniformly distributed axial load along the length and concentric axial load at free end by solving the nonlinear differential equation with the differential transformation technique. The buckling load at various slopes at free end of column is calculated and the results of the analysis using the differential transformation technique is verified with those of previous studies. It is also shown through the results that the buckling load of sinusoidal tapered columns is largest, the linear is second largest, and the parabolic is small in the all ranges of slopes at free end and the deflection of parabolic tapered columns in the x coordinates is largest, the sinusoidal is second largest, and the linear is smallest in the range of slope 0 to 140 degrees at free end. However, when the range of the slope is 160 to 176 degrees at the free end, the deflection of sinusoidal tapered columns in the x coordinates is largest, the linear is second largest, and the parabolic is smallest. In addition, for the linear tapered column, the buckling load increases along with the flexural stiffness ratio. Also, for the parabolic and the sinusoidal tapered column, the buckling loads increase and decrease as the flexural ratios increase in the range of flexural stiffness ratio $n = 1.0$ to $n = 2.0$. Through this research, it is verified that the differential transformation technique can be applied to solve the nonlinear differential equation problems, such as analysis of post-buckling behavior of tapered columns. It is also expected that the differential transformation technique apply to various more complicated problems in future.

Keywords : Tapered Columns, Combined Load, Differential Transformation, Post-buckling, Nonlinear Differential Equation

1. INTRODUCTION

Post-buckling behavior of prismatic column under a concentric axial load was analyzed by S. P. Timoshenko and J.M. Gere using an elliptical integration, which has a governing equation of large deformation[1)]. G. Venkateswara Rao and P. C. Raju performed the analysis of post-buckling behavior under uniformly loaded columns using a finite element method[2)]. For the case of uniformly load along the length and concentrically loaded at the free end, K. Lee performed the numerical analysis using the Butcher's fifth-order Runge-Kutta method[3)]. Those studies performed the analysis of post-buckling behavior of prismatic columns considering only the flexural deformation, not the shear.

In addition, Y.C. Yoo performed the numerical analysis of post-buckling behavior of prismatic columns under a combined load of uniformly distributed axial load along the length and concentric axial load at free end using the differential transformation considering not only flexural deformation but also shear deformation[4)].

* Corresponding author
Tel.:+82-54-820-5597; Fax.:+82-54-820-5860
E-mail address: ycyoo@andong.ac.kr

Previous studies stated above performed the analysis of post-buckling behavior of only prismatic columns, not tapered columns considering flexural deformation, or considering not only flexural deformation but also shear deformation.

Current research investigates the post-buckling behavior and buckling load of tapered columns under a combined load of uniformly distributed axial load along the length and concentric axial load at free end using the nonlinear differential equation and differential transformation.

2. GOVERNING EQUATIONS

As shown in Fig. 1 (a), a tapered cantilever column is loaded uniformly distributed axial force (w) along the length and concentric axial force (p) at the free end. The column is assumed to have a linear elastic, isotropic material properties and its axial deformation is negligibly small. The flexural stiffness of the column varies along the length as shown in Fig. 1 (b).

Origin (o) is set at free end in the rectangular coordinate system. The vertical axis is x-axis and the horizontal axis is y-axis. The arc length from the origin is defined s. The differential equation of the deflection can be derived as Eq. (1) using the defined coordinate system.

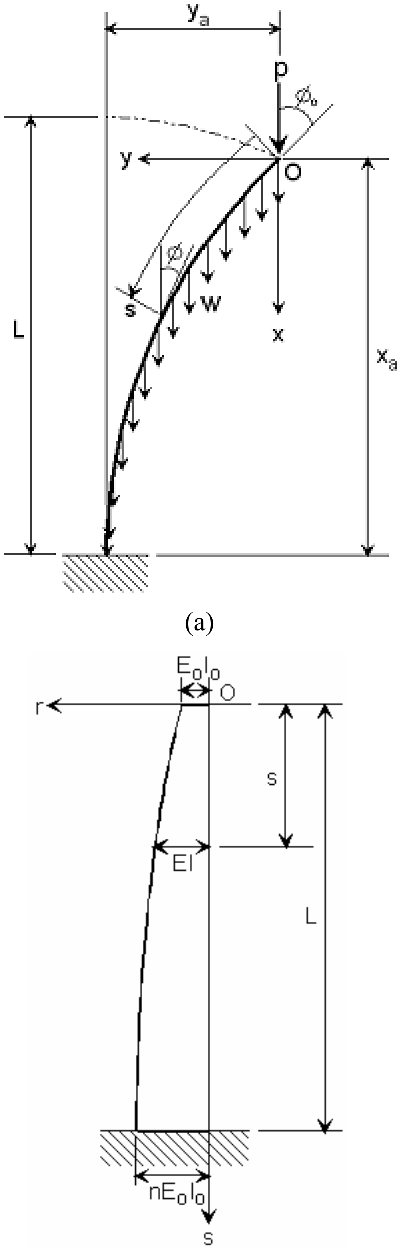

Figure 1. Column under the combined loading

$$\frac{d\phi}{ds} = \frac{M}{EI} \tag{1}$$

where, ϕ is the slope to the x-axis, M is a flexural moment, EI is a flexural stiffness.

The flexural stiffness is varied by $EI = E_0 I_0 r(s)$ along the length of the column at $s = s$. For defining geometry of column, a flexural stiffness ratio n is introduced as $n = E_0 I_0 / E_m I_m$. $E_0 I_0$ is the flexural stiffness of the column at $s = 0$ and $E_m I_m$ is the flexural stiffness of the column at $s = L$. In this study, the linear, parabolic, and sinusoidal taper are chosen as the variable flexural stiffness of the columns.

1) Linear taper

$$EI = E_0 I_0 [(n-1)\frac{s}{L} + 1]$$

2)Parabolic taper

$$EI = E_0 I_0 [-(n-1)(\frac{s}{L})^2 + 2(n-1)\frac{s}{L} + 1]$$

3)Sinusoidal taper

$$EI = E_0 I_0 [(n-1)\sin(\frac{\pi s}{2L}) + 1]$$

A flexural moment and a shear force at an arbitrary location are calculated by differentiating the Eq. (1) about s. By applying the distributed load (w) and the concentric load (p), the governing equation can be derived as follows.

$$\frac{d}{ds}[EI\frac{d\phi}{ds}] = -(p + ws)\sin\phi \tag{2}$$

The boundary conditions at free end ($s = 0$) and at fixed end ($s = L$) are follows.

$$s = 0, \phi = \phi_0 \;\&\; d\phi / ds = 0 \tag{3}$$

$$s = L, \phi = 0 \tag{4}$$

where, L is the length of column.

By introducing a new parameter $\xi = s / L$, the Eq. (2) can be nondimensionalized as Eq. (5).

$$\frac{d}{d\xi}[r(\xi)\frac{d\phi}{d\xi}] = -\frac{L^2}{E_0 I_0}(p + w\xi L)\sin\phi \tag{5}$$

By introducing the parameters $\kappa = \frac{pL^2}{EI}, \gamma = \frac{\omega L^3}{EI}$ to Eq. (5), it is derived a nondimensionalized governing differential equation that composed of the distributed uniform axial load and concentric axial load as follows.

$$r\frac{d^2\phi}{d\xi^2} + \frac{dr}{d\xi}\cdot\frac{d\phi}{d\xi} + (\kappa + \gamma\xi)\sin\phi = 0 \tag{6}$$

The boundary conditions at free end (ξ=0) and at fixed end (ξ=1) are follows.

$$\xi = 0, \phi = \phi_0 \;\&\; \frac{d\phi}{d\xi} = 0 \tag{7}$$

$$\xi = 1, \phi = 0 \tag{8}$$

Since the buckling loads (p and w) are derived from Eq. (6), this research analyzes the Eq. (6) to solve the nonlinear differential equation using the differential transformation technique.

3. Differential Transformation

The differential transformation[5)] technique was initially proposed by J. K. Zhou in 1986 using Taylor Series[6)] to solve the linear and nonlinear initial value problems in the electric circuit research. This approach can also be applied to other linear and nonlinear engineering problems using simple recursion formula and can derive high accurate solutions.

The differential transformation of arbitrary function is derived as follows.

$$Y(k) = \frac{1}{k!}\left[\frac{d^k y(x)}{dx^k}\right]_{x=0} \tag{9}$$

where, Y(k) is a differential transformed function or a T-function.

The differential inverse transformation of Y(k) is defined as follows.

$$y(x) = \sum_{k=0}^{\infty} x^k Y(k) \tag{10}$$

Using Eq. (9) and Eq. (10), the original function, y(x), can be derived as follows.

$$y(x) = \sum_{k=0}^{\infty} \frac{x^k}{k!}\left[\frac{d^k y(x)}{dx^k}\right]_{x=0} \tag{11}$$

Based on these derivations, the basic relationships of differential transformation are summarized at Table 1.

Table 1. Relationship between original and differential transformation functions

Original Functions	Differential Transformation Functions	
$w(x) = y(x) \pm z(x)$	$W(k) = Y(k) \pm Z(k)$	
$w(x) = \lambda y(x)$	$W(k) = \lambda Y(k)$	
$w(x) = \frac{d^n y(x)}{dx^n}$	W(k)=(k+1)(k+2)…(k+n)Y(k+n)	
$w(x) = y(x)z(x)$	$W(x) = \sum_{l=0}^{k} Y(l)Z(k-1)$	
$w(x) = x^m$	$W(k) = \delta(k-m)$	1 , k=m 0 , k≠m

λ : Constant, $\delta(k)$: Dirac delta function

In the practical applications, y(x) can include only finite number of terms and can be rewritten as Eq. (12).

$$y(x) = \sum_{k=0}^{m} x^k Y(k) \tag{12}$$

The number of terms (m) is decided considering the desired accuracy, and the remaining terms are negligibly small comparing to the result of calculations.

For a prismatic column under the combined axial load, the governing equation, Eq. (6) can be rewritten using the differential transformation technique as follows.

$$\sum_{l=0}^{k} R[l](k-l+1)(k-l+2)\Phi[k-l+2] + \sum_{l=0}^{k}(l+1)R[l+1](k-l+1)\Phi[k-l+1] + \kappa\Phi_s[k] + \gamma\sum_{l=0}^{k}\Phi_s[k-l]\delta[l-1] = 0 \tag{13}$$

Where, $\Phi[k]$, $\Phi_s[k]$, and $\Phi_c[k]$ are the differential transformation functions of $\phi[\xi]$, $\sin\phi[\xi]$, and $\cos\phi[\xi]$, respectively. $\delta(k)$ is the Dirac delta function.

The boundary conditions are presented as follows.

$$\xi = 0, \Phi[0] = \phi_0 \ \& \ \Phi[1] = 0 \tag{14}$$

$$\xi = 1, \sum_{k=1}^{\infty}\Phi[k] = 0 \tag{15}$$

Eq. (13) is the nonlinear equation for the computational analysis and becomes Eq.(16) when k=0.

$$\Phi[2] = -\frac{k\Phi_s[0]}{2R[0]} \tag{16}$$

For the numerical analysis, Eq. (13) is rewritten as Eq. (17) for integer m and $k \geq 1$.

$$\Phi[k+2] = -\{\sum_{l=1}^{k} R[l](k-l+1)(k-l+2)\Phi[k-l+2] + \sum_{l=0}^{k}(l+1)R[l+1](k-l+1)\Phi[k-l+1] + \kappa\Phi_s[k] + \gamma\sum_{l=0}^{k}\Phi_s[k-1]\} / \{R[0](k+1)(k+2)\} \tag{17}$$

Applying the equations, $\Phi[0] \sim \Phi[k]$, to Eq.(15), the equation for the buckling load, Eq. (18), is derived.

$$f^{(k)}(Q^{(k)}) = 0 \tag{18}$$

where, $Q^{(k)}$ is a polynominal of k, which has variables κ, and γ.

From Eq. (18), ith buckling load $Q = Q_i^{(k)}$ (i=1, 2, ⋯) is calculated about k, which is decided from Eq. (19).

$$\left|Q_i^{(k)} - Q_i^{(k-1)}\right| \leq \varepsilon \tag{19}$$

where, $Q_i^{(k-1)}$ is the ith buckling load about (k-1) and ε is an allowable error.

The finite series for $Q_i^{(k)}$ is rewritten from Eq. (12) by applying $\Phi[0] \sim \Phi[k]$, which the $Q_i^{(k)}$ is applied to.

$$\phi_i(\xi) = \sum_{k=0}^{n} \xi^k \Phi(k) \tag{20}$$

where, $\phi_i(\xi)$ is the slope of ith buckling mode of a column under a combined load at the nondimensionalized buckling load $Q_i^{(k)}$.

Using the slope (ϕ), which is a function of an nondimensionalized buckling load and ξ, the x and y coordinates of the deflected shape are calculated in Eqs. (21) and (22) respect to the neutral axis of the column.

$$x(\xi) = L\int_0^{\xi} \cos\phi d\xi \tag{21}$$

$$y(\xi) = L\int_0^{\xi} \sin\phi d\xi \tag{22}$$

4. ANALYSIS RESULTS

Since the differential transformation is a transformation technique based on the Taylor series, the result of analysis is described in the form of infinite series. These results can be solved easily using the mathematical software packages. Mathematica Version 4.2[7] for MS Windows of Wolfram Research, Inc. is used for this purpose.

Table 2. Comparison of buckling load(κ) of column when only concentric axial load(p) is applied at free end. $(\kappa = pL^2 / EI)$

ϕ (deg.)	Analysis Result	Elliptical Integration[1]	5th order Runge Kutta[3]
0	2.4674	2.4674	2.4671
20	2.5057	2.5044	2.5049
40	2.6238	2.6228	2.6240
60	2.8360	2.8424	2.8412
80	3.1815	3.1903	3.1920
100	3.7506	3.7455	3.7458
120	4.7418	4.6486	4.6498
140	6.5755	6.2697	6.2719
160	10.2282	9.9412	9.9428
176	40.7759	22.4928	-

Note: The number of terms used in the differential transformation series is 11.

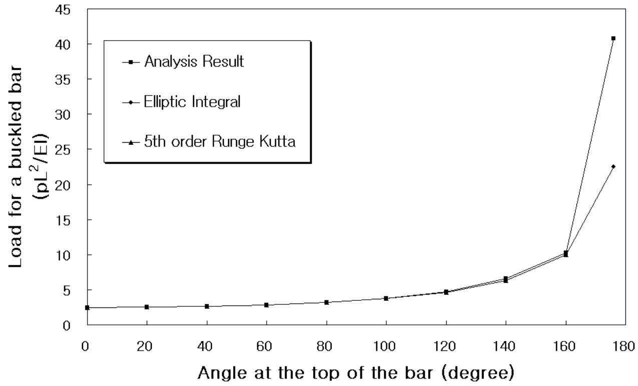

Figure 2. Relation of buckling load and free-end slope when only concentric axial load(p) is applied at free end

Three different loading conditions are considered for the analysis of post-buckling behavior of column. These cases are a concentric axial load only, uniformly distributed axial load only, and the combination of previous two load cases.

In order to verify the results of current research about the loading conditions, the analysis is performed about the prismatic columns. Tables 2 to 7 and figures 2 to 7 show the buckling load and deflection of the prismatic columns about various slope at the free end.

Table 3. Comparison of free-end-deflection of column when only concentric axial load(p) is applied at free end. $(\kappa = pL^2 / EL)$

ϕ (deg.)	Analysis Result		Elliptic Integral[1]		5th order Runge Kutta[3]	
	x_a/L	y_a/L	x_a/L	y_a/L	x_a/L	y_a/L
0	1.0000	0.0000	1.0000	0.0000	1.0000	0.0000
20	0.9697	0.2194	0.9700	0.2200	0.9698	0.2194
40	0.8812	0.4223	0.8810	0.4220	0.8812	0.4223
60	0.7408	0.5937	0.7410	0.5930	0.7410	0.5933
80	0.5587	0.7205	0.5600	0.7190	0.5594	0.7196
100	0.3492	0.7913	0.3490	0.7920	0.3490	0.7916
120	0.1303	0.7983	0.1230	0.8030	0.1231	0.8032
140	-0.0870	0.7408	-0.1070	0.7500	-0.1070	0.7505
160	-0.3491	0.6218	-0.3400	0.6250	-0.3404	0.6247
176	-0.7338	0.3257	-0.5770	0.4210	-	-

Note: The number of terms used in the differential transformation series is 11.

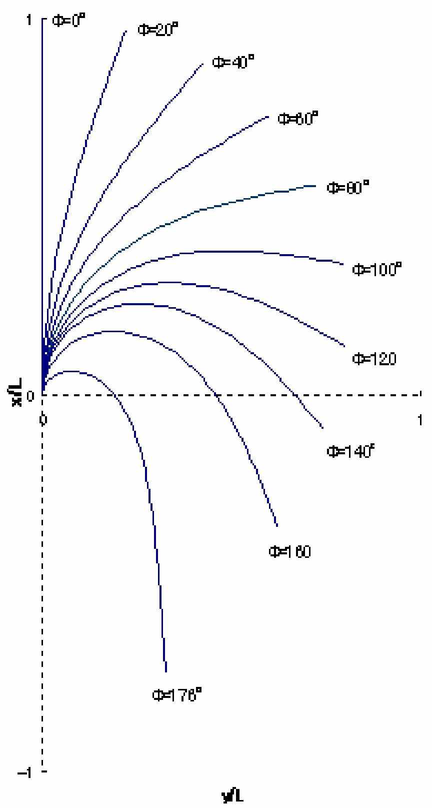

Figure 3. Nondimensionalized deflection when only concentric axial load (p) is applied at free end

Table 4. Comparison of buckling load(γ) of column when only uniformly distributed axial load(w) is applied. $(\gamma = wL^3 / EI)$

ϕ (deg.)	Analysis Result	5th order Runge Kutta[3)]
0	7.8373	7.8356
20	7.9497	7.9448
40	8.2868	8.2877
60	8.8754	8.9101
80	9.8394	9.9070
100	11.4827	11.4638
120	14.4542	13.9685
140	19.8382	18.3809
160	28.5646	28.1280
176	105.3010	-

Note: The number of terms used in the differential transformation series is 16.

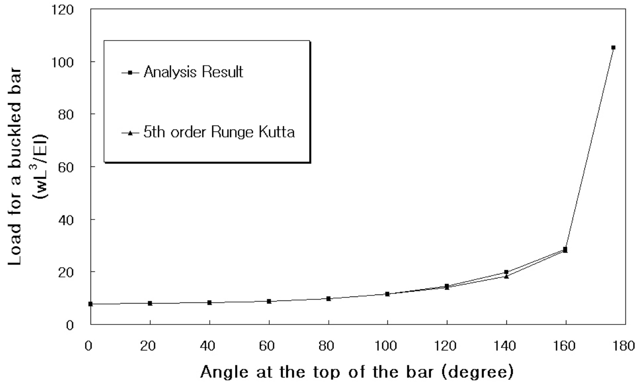

Figure 4. Relation of buckling load and free-end slope when only uniformly distributed axial load (w) is applied

Also, the analysis of tapered columns is performed in the range of flexural stiffness ratio $n = 1.0$ to $n = 2.0$. Tables 8 to 9 and figures 8 to 9 summarize the analysis results of the tapered columns to investigate the influence of the variation of flexural stiffness to the buckling load in the case of a flexural stiffness ratio $n = 1.5$.

As shown in tables 2 to 7 and figures 2 to 7, the current results about the prismatic columns show the similar results of previous research, which are analytical studies using elliptical integration and numerical studies using Butcher's 5th order Runge-Kutta method.

Table 5. Comparison of free-end-deflection of column when only uniformly distributed axial load(w) is applied. $(\gamma = wL^3 / EI)$

ϕ (deg.)	Analysis Result		5th order Runge Kutta[3)]	
	x_a / L	y_a / L	x_a / L	y_a / L
0	1.0000	0.0000	1.0000	0.0000
20	0.9631	0.2484	0.9685	0.2255
40	0.8564	0.4732	0.8761	0.4336
60	0.6878	0.6589	0.7299	0.6082
80	0.4717	0.7878	0.5406	0.7358
100	0.2282	0.8459	0.3216	0.8063
120	-0.0173	0.8249	0.0872	0.8130
140	-0.2489	0.7276	-0.1502	0.7517
160	-0.5191	0.5630	-0.3877	0.6133
176	-0.8213	0.2500	-	-

Note: The number of terms used in the differential transformation series is 16.

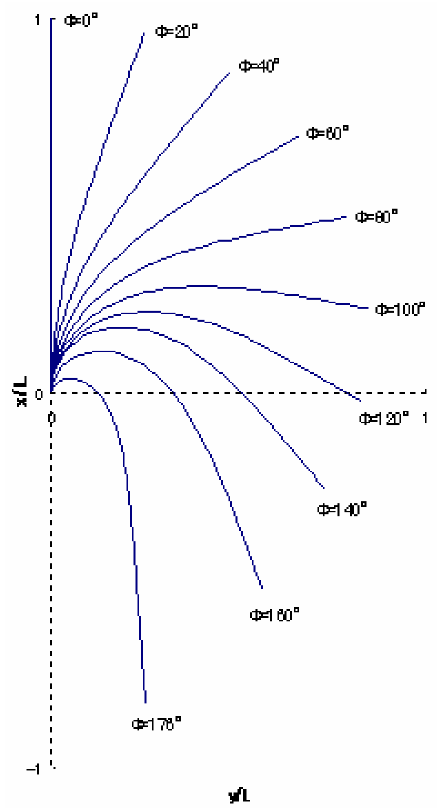

Figure 5. Nondimensionalized deflection when only uniformly distributed axial load(w) is applied along the length

Table 6. Comparison of buckling load(κ and γ) of column when a combination of concentric axial load(p) and uniformly distributed axial load(w) is applied. $(\kappa = \gamma = pL^2 / EI = wL^3 / EI)$

ϕ (deg.)	Analysis Result	5th order Runge Kutta[3)]
0	1.8959	1.8957
20	1.9228	1.9237
40	2.0098	2.0120
60	2.1758	2.1726
80	2.4561	2.4309
100	2.9089	2.8368
120	3.6137	3.4948
140	4.6994	4.6649
160	7.0633	7.2815
176	29.9863	-

Note: The number of terms used in the differential transformation series is 16.

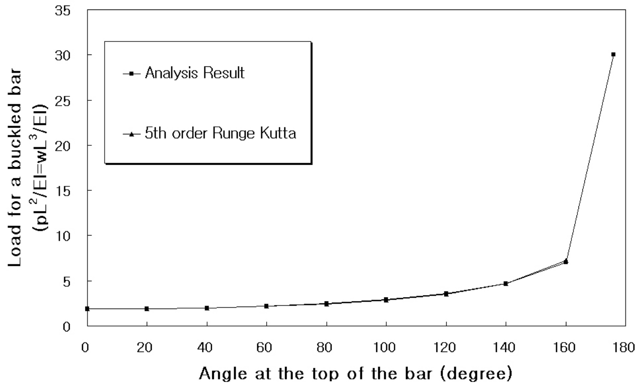

Figure 6. Relation of buckling load and free-end slope when a combination of concentric axial load(p) and uniformly distributed axial load(w) is applied

The buckling load at 176 degree of slope shows a discrepancy from the elliptical analysis. This is because the geometric nonlinearity according to the increment of the slope at free end. It is considered to be reduced the difference by increasing the number of terms in the finite series of the differential transformation.

Tables 8 to 9 and figures 8 to 9 show the buckling load and deflection of the tapered columns about various slope at the free end in the case of a flexural stiffness ratio $n = 1.5$. As shown in table 8, the buckling load of sinusoidal tapered columns is largest, the linear is second largest, and the parabolic is smallest in the all ranges of slopes at free end.

Table 7. Comparison of free-end-deflection of column when a combination of concentric axial load(p) and uniformly distributed axial load(w) is applied. $(\kappa = \gamma = pL^2 / EI = wL^3 / EI)$

ϕ (deg.)	Analysis Result		5th order Runge Kutta[3)]	
	x_a / L	y_a / L	x_a / L	y_a / L
0	1.0000	0.0000	1.0000	0.0000
20	0.9684	0.2256	0.9634	0.2473
40	0.8760	0.4338	0.8564	0.4732
60	0.7300	0.6080	0.6882	0.6582
80	0.5425	0.7333	0.4729	0.7864
100	0.3287	0.7998	0.2279	0.8462
120	0.0995	0.8050	-0.0277	0.8312
140	-0.1496	0.7503	-0.2763	0.7392
160	-0.4258	0.6129	-0.5083	0.5657
176	-0.7525	0.3092	-	-

Note: The number of terms used in the differential transformation series is 16.

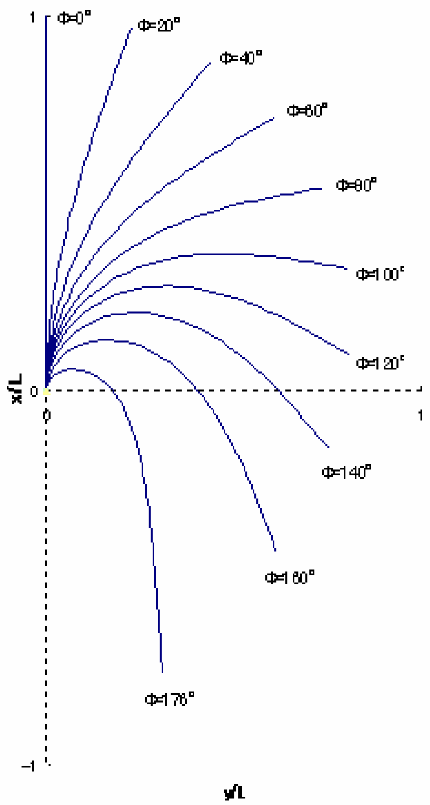

Figure 7. Nondimensionalized deflection when a combination of concentric axial load(p) and uniformly distributed axial load(w) is applied

Next, as shown in table 9, the deflection of parabolic tapered columns in the x coordinates is largest, the sinusoidal is second largest, and the linear is smallest in the range of slope 0 to 140 degrees at free end. However, when the range of the slope is 160 to 176 degrees at the free end, the deflection of sinusoidal tapered columns in the x coordinates is largest, the linear is second largest, and the parabolic is smallest.

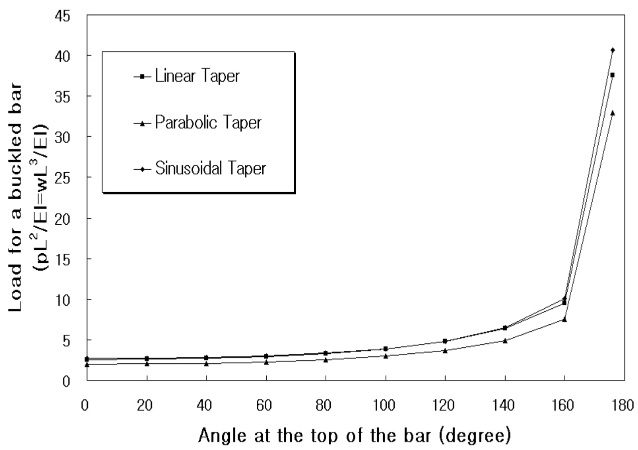

Figure 8. Relation of buckling load and free-end slope when a combination of concentric axial load(p) and uniformly distributed axial load(w) is applied. (tapered column, $n = 1.5$)

Figures 10 (a), (b), and (c) show the relation of buckling load, $pL^2 / EI = wL^3 / EI$, and flexural stiffness ratio, n, for the linear, parabolic, and sinusoidal tapered column, respectively.

As shown in figures 10, for the linear taper, the buckling load increases along with the flexural stiffness ratio. Also, for the parabolic taper and the sinusoidal taper, the buckling loads increase and decrease as the flexural ratios increase. For the case of the parabolic taper, the strongest column occurs at the flexural ratio, $n = 1.6$ as shown in figures 10 (b). For the case of the sinusoidal taper, the strongest column occurs at the flexural ratio, $n = 1.9$, or $n = 1.7$, for the range of slope 0 to 80 degrees, 176 degrees at free end, respectively as shown in figures 10 (c).

This research shows the possibility of analysis using the differential transformation about a tapered column, which has arbitrary flexural stiffness as well as the chosen flexural stiffness, the linear, parabolic, and sinusoidal taper, for the various applied load as shown above. It is also possible to analyze the column for the various linear load combination using the relation of $\kappa = c\gamma$, where c is constant.

Table 8. Comparison of buckling load (κ and γ) of column when a combined load of concentric axial load (p) and uniformly distributed axial load (w) is applied. ($\kappa = pL^2 / EI = wL^3 / EI$, tapered column, $n = 1.5$)

ϕ (deg.)	Linear Taper	Parabolic Taper	Sinusoidal Taper
0	2.5672	1.9783	2.6887
20	2.6040	2.0080	2.7256
40	2.7183	2.1015	2.8368
60	2.9264	2.2737	3.0311
80	3.2704	2.5538	3.3465
100	3.8409	2.9945	3.8739
120	4.8146	3.6895	4.7987
140	6.4430	4.8529	6.4969
160	9.5193	7.4918	10.0466
176	37.5779	32.9710	40.6778

Note: The number of terms used in the differential transformation series is 16.

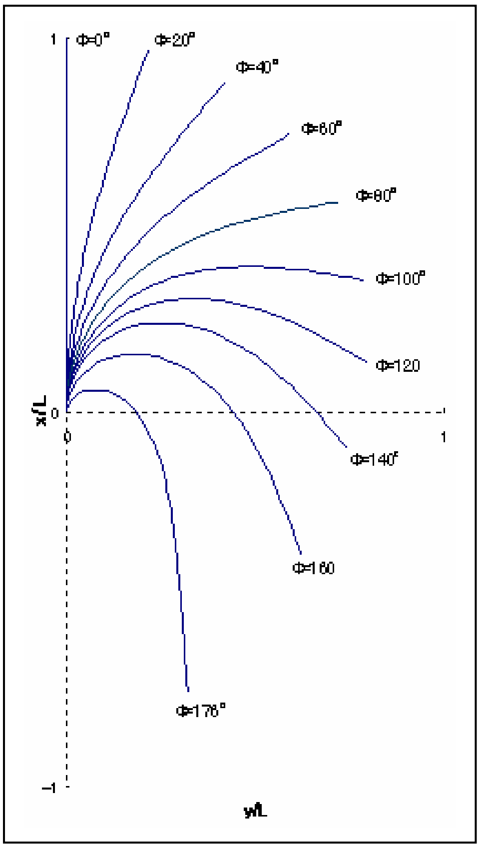

(a) linear taper

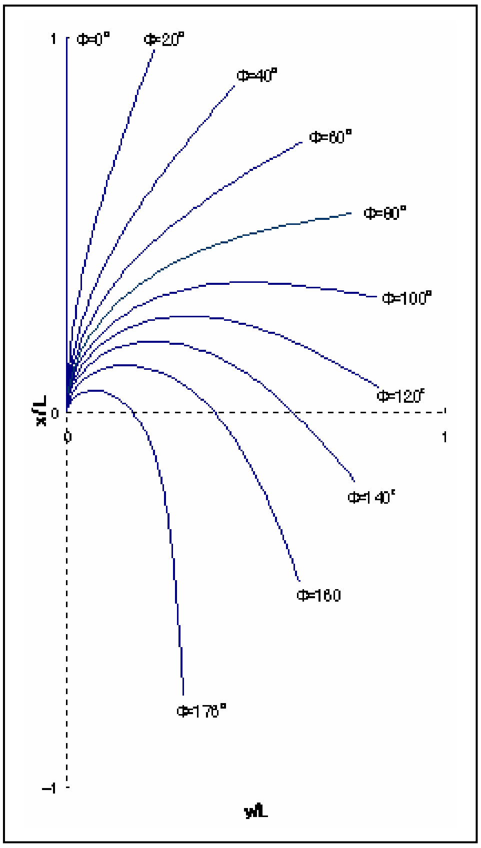

(b) Parabolic taper

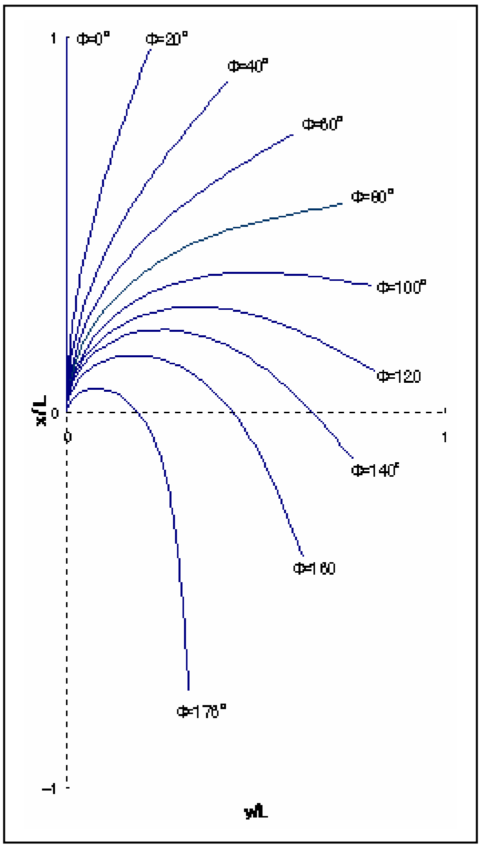

(c) sinusoidal taper

Figure 9. Nondimensionalized deflection when a combination of concentric axial load(p) and uniformly distributed axial load(w) is applied. ($\kappa = pL^2 / EI = wL^3 / EI$, tapered column, $n = 1.5$)

Table 9. Comparison of nondimensionalized deflection at free end when a combined load of concentric axial load (p) and uniformly distributed axial load (w) is applied. ($\kappa = pL^2 / EI = wL^3 / EI$, tapered column, $n = 1.5$)

ϕ (deg.)	Linear Taper		Parabolic Taper		Sinusoidal Taper	
	x_a / L	y_a / L	x_a / L	y_a / L	x_a / L	y_a / L
0	1.0000	0.0000	1.0000	0.0000	1.0000	0.0000
20	0.9702	0.2171	0.9677	0.2301	0.9699	0.2189
40	0.8827	0.4182	0.8731	0.4422	0.8815	0.4223
60	0.7438	0.5887	0.7237	0.6197	0.7403	0.5959
80	0.5635	0.7149	0.5308	0.7483	0.5550	0.7266
100	0.3560	0.7854	0.3087	0.8179	0.3393	0.8016
120	0.1380	0.7929	0.0698	0.8235	0.1108	0.8113
140	-0.0910	0.7406	-0.1807	0.7614	-0.1194	0.7537
160	-0.3742	0.6213	-0.4462	0.6139	-0.3814	0.6232
176	-0.7396	0.3200	-0.7544	0.3087	-0.7362	0.3226

Note: The number of terms used in the differential transformation series is 16.

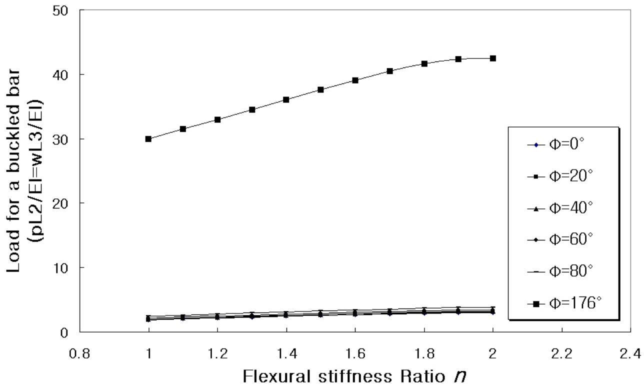

(a) Linear taper

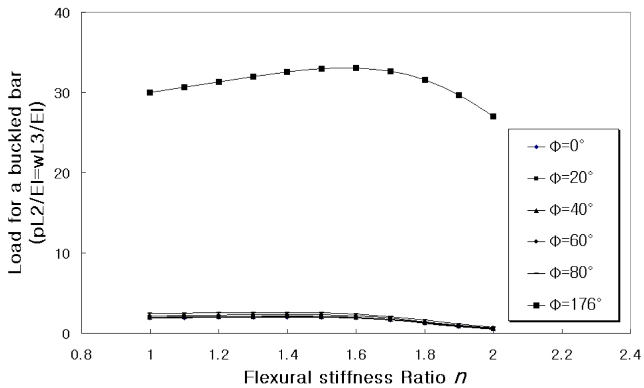

(b) Parabolic taper

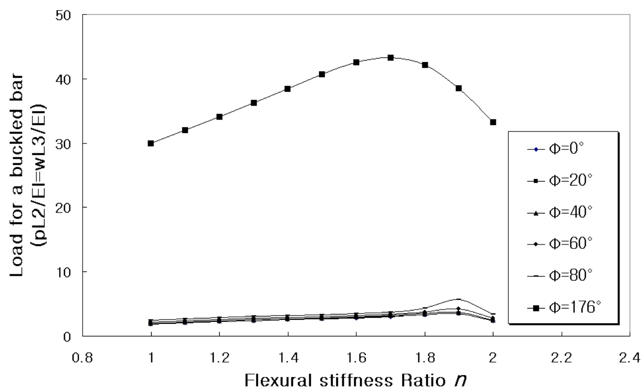

(c) Sinusoidal taper

Figure 10. Relation of buckling load and flexural stiffness ratio when a combination of concentric axial load(p) and uniformly distributed axial load(w) is applied

5. CONCLUSION

This research calculated the buckling load of tapered column and analyzed the post-buckling behavior by solving the nonlinear differential equation using the differential transformation technique. The load combinations considered are a concentric load at free end, a uniformly distributed load along the length, and a combined load of concentric load and uniformly distributed load. The variation of flexural stiffness is included in the nonlinear differential equation.

The analysis results using the differential transformation verify with the results of previous studies. The buckling load of sinusoidal tapered columns is largest, the linear is second largest, and the parabolic is smallest in the all ranges of slopes at free end.

This research provided the possibility of the analysis of post-buckling behavior for the various flexural stiffness, and load conditions using the differential transformation technique. It is also possible to extend the linear combinations of loads.

Through this research, it is verified that the differential transformation technique can apply to solve the nonlinear differrential equation problems, such as analysis of post-buckling behavior. It is also expected that the differential transformation technique apply to various more complicated problems in the future.

ACKNOWLEDGEMENT

This work was supported by the Research Project of Andong National University in 2003. This support is gratefully acknowledged.

REFERENCES

S. P. Timoshenko and J. M. Gere, “Theory of Elastic Stability”, McGraw-Hill, New York, 1961, pp. 76-81.

G. Venkateswara Rao and P. C. Raju, “Post-buckling of uniform cantilever column - Galerkin finite element solution”, Engng. Fract. Mechanics, 1977, 1-4.

Kyungwoo Lee, “Post-buckling of uniform cantilever column under a combined load”, International Journal of Non-Linear Mechanics, Vol. 36, 2001, pp. 813-816.

Yeongchan Yoo (2004) “Post-Buckling Behavior of Shear-Deformable Prismatic Columns Under a Combined Load using Differential Transformation”, Journal of the Architectural Institute of Korea, Vol. 6, 2004, pp. 31-42.

J. K. Zhou, “Differentional Transformation and Its Applications for Electrical Circuits”, Huazhong University Press, 1986.

Thomas and Finney, “Calculus and Analytic Geometry”, Addison-Wesley, New York, 1961, pp. 594-614.
Mathematica Version 4.2 For Microsoft Windows, Wolfram Research, Inc.
Chao-Kuang Chen and Shing-Huei Ho, “Application of Differentional Transformation to Eigenvalue Problems”, Applied Mathematics and Computation, Vol. 79, 1996, pp. 173-188.
B.K. Lee and S.J. Oh, “Elastica and buckling load of simple tapered columns with constant volume”, International Journal of Solids and Structures, Vol. 37, 2000, pp. 2507-2518.
David Goeken and Olin Johson, “Fifth-order Runge-Kutta with Higher Order Derivative Approximations”, Electric Journal of Differential Equations, Conference 02, 1999, pp. 1-9.

(Data of Submission : 2006. 2.10)